A COMPACT TORUS PLASMA FLOW SWITCH

Robert E. Peterkin, Jr.
Mission Research Corporation
1720 Randolph Road, SE, Albuquerque, NM 87106 USA

James H. Degnan, Norman F. Roderick, and Carl R. Sovinec
Phillips Laboratory, Kirtland Air Force Base, NM 87117 USA

Peter J. Turchi
Department of Aeronautical and Astronautical Engineering
The Ohio State University, Columbus, OH 43210 USA

Abstract

Experiments to form and accelerate compact toroid (CT) plasmas have been performed on the 9.4 MJ Shiva Star fast capacitor bank at Phillips Laboratory (Kirtland AFB, New Mexico) since late 1990. In this paper, we investigate the possibility of employing a CT as a very fast opening switch to drive fast Z-pinches by performing a series of 2 1/2-dimensional magnetohydrodynamic computer simulations. Comparisons are made between computer simulations of conventional and compact torus plasma flow switches. We find that a CT switch leaves less switch plasma on the electrode walls, and can deliver current to an implosion load faster and more uniformly than a conventional plasma flow switch.

Introduction

The MARAUDER (Magnetically Accelerated Rings to Achieve Ultrahigh Directed Energy and Radiation) program[1] is a research effort to accelerate magnetized plasma rings with masses between 0.1 and 1.0 mg to velocities above 100 cm/μs and energies above 1 MJ. Research on these high-velocity compact toroids may lead to development of very fast opening switches, intense X-ray sources, high-power microwave sources, and an alternative path to inertial confinement fusion.

In this paper, we discuss the possibility of employing a CT plasma as a very fast opening switch to drive fast Z-pinches. In the 1980-s, the Shiva Star capacitor bank and an inductive store were used to drive Z-pinches with mulitmegaampere currents and sub-microsecond rise times.[2,3] In these earlier experiments, magnetic energy was stored in a vacuum inductor behind a conventional plasma flow switch (PFS) of the type designed by Turchi and coworkers.[4,5] The particular PFS used in the earlier Shiva Star experiments was an annular armature that was constructed of a chordal array of aluminum wires upstream of a thin plastic film. The wires conduct electric current between coaxial electrodes and subsequently accelerate down the coaxial gun as a plasma armature. It is useful to think of the magnetic energy behind the PFS as a magnetic piston that exerts a pressure on the armature. The geometry of a conventional PFS and implosion foil from the Quick Fire series of experiments performed in 1984–85 on Shiva Star[6] is shown in Figure 1. The switch opens as the discharge sweeps off the end of the center conductor and transfers energy to a load—in the present case a cylindrical implosion foil. The time interval that is required for a conventional PFS to traverse an axial gap in the center conductor determines, to first order, the current rise time in the cylindrical load foil. High speed, low density plasma behind the discharge convects the magnetic energy that is stored behind the PFS to the load.

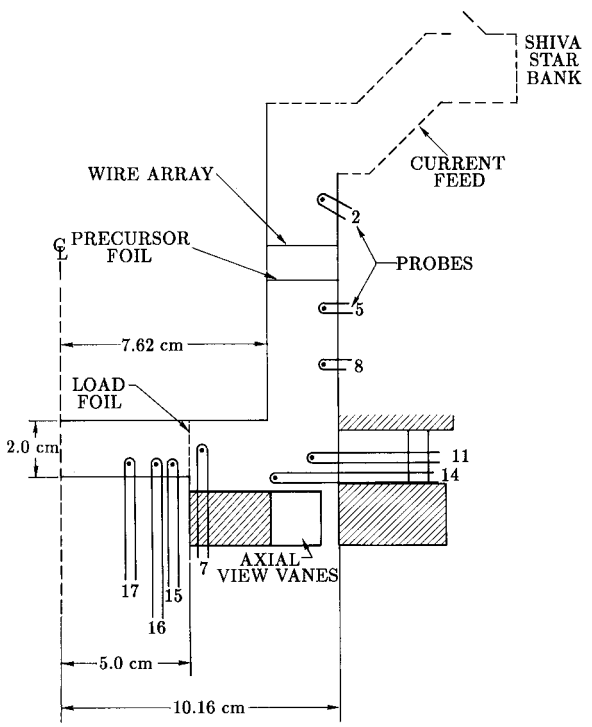

Figure 1. Schematic of a conventional PFS and implosion foil from the Quick Fire series of experiments at Phillips Laboratory. The dashed area is not to scale.

The earlier fast Z-pinch program was quite successful. Through a combined experimental and theoretical effort, between 80–100% of the full 12 MA produced by Shiva Star with 4.6 MJ of stored energy were delivered to an implosion foil.[7,8] The implosion foils radiated between 400–900 kJ at a peak power between 3–6 TW as it stagnated on the symmetry axis.[2,8,9] The conventional PFS, however, is not perfect, and it is our conjecture that a CT PFS may perform even better.

There is a tendency for a conventional PFS armature to spread axially as the acceleration time increases, so a higher velocity does not necessarily imply a shorter transit time across the axial gap. In addition, not all of the mass of the PFS is driven out of the switch region, but rather some of the mass remains on the electrode walls and moves at a lower speed than the bulk of the switch mass. The mass that is left on the electrodes has the deleterious effect of slowing the rate at which energy is convected to the load after the switch opens. It may be possible, however, to confine the high-density armature in a magnetic "bag" by embedding the plasma in a "force-free" magnetic structure that moves at its Alfvén speed. Such a

Report Documentation Page

Form Approved
OMB No. 0704-0188

1. REPORT DATE	2. REPORT TYPE	3. DATES COVERED
JUN 1991	**N/A**	**-**

4. TITLE AND SUBTITLE	5a. CONTRACT NUMBER
A Compact Torus Plasma Flow Switch	5b. GRANT NUMBER
	5c. PROGRAM ELEMENT NUMBER
6. AUTHOR(S)	5d. PROJECT NUMBER
	5e. TASK NUMBER
	5f. WORK UNIT NUMBER
7. PERFORMING ORGANIZATION NAME(S) AND ADDRESS(ES) **Mission Research Corporation 1720 Randolph Road, SE, Albuquerque, NM 87106 USA**	8. PERFORMING ORGANIZATION REPORT NUMBER
9. SPONSORING/MONITORING AGENCY NAME(S) AND ADDRESS(ES)	10. SPONSOR/MONITOR'S ACRONYM(S)
	11. SPONSOR/MONITOR'S REPORT NUMBER(S)

12. DISTRIBUTION/AVAILABILITY STATEMENT
Approved for public release, distribution unlimited

13. SUPPLEMENTARY NOTES
See also ADM002371. 2013 IEEE Pulsed Power Conference, Digest of Technical Papers 1976-2013, and Abstracts of the 2013 IEEE International Conference on Plasma Science. Held in San Francisco, CA on 16-21 June 2013. U.S. Government or Federal Purpose Rights License.

14. ABSTRACT
Experiments to form and accelerate compact toroid (CT) plasmas have been performed on the 9.4 MJ Shiva Star fast capacitor bank at Phillips Laboratory (Kirtland AFB, New Mexico) since late 1990. In this paper, we investigate the possibility of employing a CT as a very fast opening switch to drive fast Z-pinches by performing a series of 2 1/2-dimensional magnetohydrodynamic computer simulations. Comparisons are made between computer simulations of conventional and compact torus plasma flow switches. We find that a CT switch leaves less switch plasma on the electrode walls, and can deliver current to an implosion load faster and more uniformly than a conventional plasma flow switch.

15. SUBJECT TERMS

16. SECURITY CLASSIFICATION OF:			17. LIMITATION OF ABSTRACT	18. NUMBER OF PAGES	19a. NAME OF RESPONSIBLE PERSON
a. REPORT	b. ABSTRACT	c. THIS PAGE			
unclassified	**unclassified**	**unclassified**	**SAR**	**6**	

configuration is less likely to elongate during the rundown phase of a plasma flow switch, and should remove most of the switch plasma from the axial gap leaving only a very low density plasma behind the main discharge to quickly convect energy to the implosion load. The rate at which energy is delivered to the surface of a load is equal to the Poynting flux, $\vec{S} = \vec{E} \times B/\mu_0$, which for high magnetic Reynolds number flows reduces to $\vec{S} = \vec{v}(B^2/\mu_0)$. In this case, magnetic energy $(B^2/2\mu_0)$ is convected with the plasma at a characteristic speed, v. The high velocities and compact nature of accelerated CT plasmas suggest that a faster and cleaner path across the axial gap, as well as more rapid energy transfer to a load foil, should be possible with a CT PFS than with conventional PFS. This, in turn, should allow greater pulse-compression than has been obtained to date with conventional PFS technology.

Numerical simulations of a CT plasma acting as a flow switch are compared to numerical simulations of a conventional wire array PFS in this paper. The simulations are performed with MACH2,[10,11] a 2 1/2-dimensional magnetohydrodynamics (MHD) simulation code for problems with complex geometry. It has been used successfully to model the conventional plasma flow switch/fast Z-pinch experiment with Shiva Star parameters.[7,9] Figure 1 is a drawing of a conventional PFS, complete with a foil implosion load. The axial view vanes at the bottom allow the plasma armature to leave the switch, serve as a current path after switching, and provide diagnostic access. Locations of the magnetic probes are also illustrated.

The compact toroids are produced in a magnetized coaxial plasma gun, and the acceleration occurs in a configuration similar to a coaxial railgun. Quasistatic compression of a CT in a coaxial geometry has been demonstrated in the RACE experiment at LLNL.[13] Detailed calculations of the formation of CT plasmas with MARAUDER parameters have been performed with MACH2.[14] When begun with realistic initial data on a computational mesh that is an image of an axisymmetric cross-section of the experiment, the code models magnetic reconnection and the formation of a CT. The numerical simulations produce magnetic probe data that can be directly compared to experimental data, and agreement is good. Additional computer simulations of the formation and subsequent acceleration of MARAUDER CT plasmas have been preformed with MACH2[15] and agreement is satisfactory.[16]

Resistive Magnetohydrodynamics

The MACH2 code solves the dynamic single-fluid MHD equations on a mesh composed of arbitrarily shaped quadrilateral cells. It is an arbitrary Lagrangian Eulerian (ALE) code with great flexibility. Logically rectangular collections of cells form finite elements that are called blocks. The blocks can be patched together to form an image of the cross section of an experiment. All three components of vector fields (fluid velocity, magnetic induction, current density, *etc.*) are carried by the code.

The equations are closed with an equilibrium equation of state (SESAME tables at Los Alamos National Laboratory) including constitutive relations for transport coefficients (conductivities and the opacity). The electrons and ions are not assumed to be in equilibrium. Thermal conduction, magnetic diffusion, and radiation cooling are included in the simulations.

The plasma is assumed to be optically thin. The mean Planck opacity is used to obtain the correct integrated value for thermal emission in the thin limit. The energy radiated during a single time step is accumulated for all cells near the implosion region, and that is used to compute the equivalent isotropic radiated power.

Initial Data for the CT PFS simulations

Numerical simulations of an entire compact torus PFS experiment, including formation, acceleration and switching from realistic initial data, have not yet been performed. Before we undertake an equivalent experiment, we decided that a numerical study to investigate the viability of the idea would be prudent. In this paper, the first step of the numerical study is presented as we address the question of how a CT PFS would perform under the most favorable formation conditions. Therefore, rather than compute the formation and compression of a CT from realistic initial data, the simulations discussed here begin with an ideal "force-free" magnetic configuration that surrounds a specific mass distribution in a plasma gun identical to that used in earlier PFS work.

The "force-free" magnetic configuration represents a solution to the vector Helmholtz equation:

$$\nabla \times \left(\nabla \times \vec{B}\right) = \alpha^2 \vec{B} \tag{1}$$

subject to the boundary conditions. An axisymmetric solution of fixed length with toroidal symmetry in which the field is tangent to the boundary and in which the azimuthal component of the field vanishes at the boundary is:

$$\begin{aligned} B_r &= \frac{B_0}{\sqrt{1+\frac{\lambda^2}{k^2}}} \cos\left(k\left(z-z_0\right)\right)\left[J_1\left(\lambda r\right) + f\, N_1\left(\lambda r\right)\right] \\ B_z &= -\frac{B_0}{\sqrt{1+\frac{\lambda^2}{k^2}}} \left(\frac{\lambda^2}{k^2}\right) \sin\left(k\left(z-z_0\right)\right)\left[J_0\left(\lambda r\right) + f\, N_0\left(\lambda r\right)\right] \\ B_\theta &= -B_0 \sin\left(k\left(z-z_0\right)\right)\left[J_1\left(\lambda r\right) + f\, N_1\left(\lambda r\right)\right] \end{aligned} \tag{2}$$

where J and N are respectively Bessel functions of the first and second kind and $\lambda^2 \equiv \alpha^2 - k^2$ where k is the axial wave number. This magnetic configuration is not an equilibrium for the geometry of Figure 2 because it is not confined by conductors at its top and bottom. The demand that B_z vanish at $z = z_m$ implies that $k = m\pi/(y_m - y_0) = 1.237$ cm^{-1} for $m = 1$ and a height of 2.54 cm. The inner radius of the gun is 7.62 cm (3 inches) and the distance between the inner and outer electrodes is 2.54 cm (1 inch). The boundary conditions at the inner (r_i) and outer (r_o) electrodes imply that

$$J_1\left(\lambda r_i\right)\, N_1\left(\lambda r_0\right) - J_1\left(\lambda r_0\right)\, N_1\left(\lambda r_i\right) = 0 \tag{3}$$

where the s-th zero of this cross product of Bessel functions has an asymptotic expansion.[17] For the geometry of Figure 1, $\lambda = 1.241$ cm^{-1}; hence, the coefficient, f, in Eq. 2. is -0.89.

The CT provides a conduction path between the coaxial electrodes that form an inductive store. The magnetic energy behind the CT acts as a piston as it performs work on the CT and drives it down the gun.

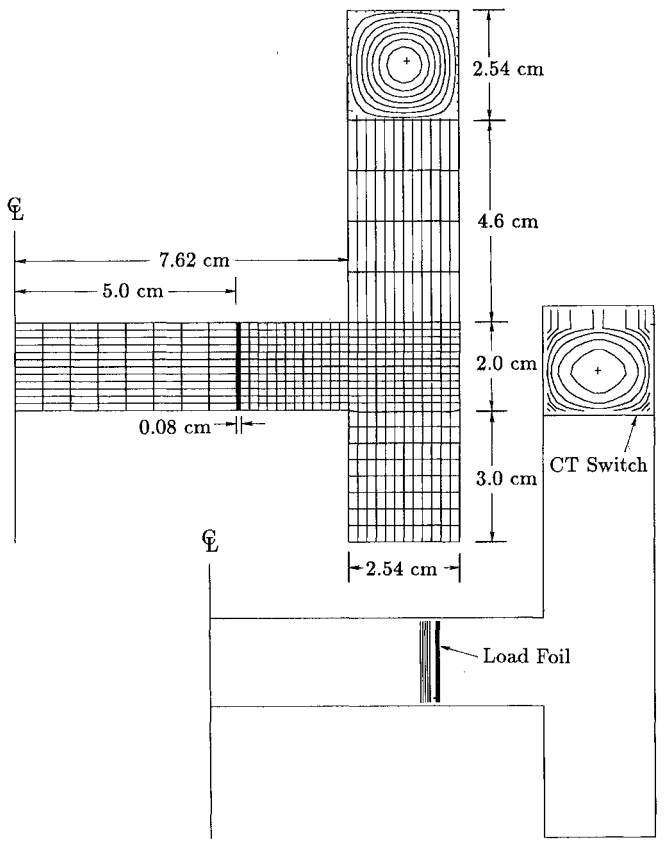

Figure 2. Initial MACH2 computational grid and initial poloidal magnetic field (above), and mass distribution (below) of the CT PFS simulations.

The mass of the Aluminum wire array in a conventional PFS used previously in the Quick Fire series of experiments is on the order of 116 mg and is distributed approximately as $1/r^2$ to yield nearly uniform axial acceleration from the magnetic piston pressure that also varies as $1/r^2$. The initial exploded wire plasma has a temperature of 1.5 eV and a center of mass axial speed of 0.584 cm/μs. The mass of the CT plasma is chosen to be 10% of the mass of the conventional PFS and is not distributed as $1/r^2$ but rather conforms to the shape of the poloidal magnetic flux surfaces. The initial magnetic field and mass distributions of the CT PFS simulation are illustrated in Figure 2.

If the magnetic piston is initially super-Alfvénic, the CT undergoes a dramatic axial compression which in turn causes the CT to contract radially. This allows the discharge to blow by the CT and the CT plasma is left in the gun. The mass left in the gun seriously degrades the performance of the switch. To avoid this difficulty, we have assumed that at $t = 0$, the magnetic piston has already accelerated the CT to its local Alfvén speed ($B_\theta/\sqrt{\mu_0\,\rho}$). Although both B_θ and ρ vary within the CT, the distributions are such that the Alfvén speed is nearly uniform throughout and is substantially greater than the initial speed of the conventional PFS. (The initial axial speed of the CT is 14 cm/μsec versus a final speed for the conventional PFS of 7 cm/μsec).

In these calculations, the initial background density is 5×10^{-7} gm/cm^3. Plasma at 1/5 this density continuously flows through the boundary upstream of the initial CT position. The toroidal magnetic field peaks in the center of the CT at an initial value of 11 T; the poloidal field reaches a maximum value of 8.4 T at the conducting walls. The total magnetic energy is 9 kJ. The PFS is assumed to be driven by the 1300 μF Shiva Star fast capacitor bank charged to 83.6 kV (4.54 MJ or half the maximum bank energy) with an external inductance of 18.79 nH. The conventional PFS simulation begins when the bank current has risen to 6.5 MA. Because the CT PFS is assumed to be moving much faster than the conventional PFS at the beginning of the simulation, the $\dot{L}$ is larger for the CT switch. A self-consistent circuit model from this state predicts that the current never rises above the initial 6.5 MA value. Hence, the energy available for delivery to a load would be significantly less than that of the conventional PFS which allows the bank to produce 10–12 MA. Therefore, the CT PFS simulation begins with the bank current at 11 MA and the remaining bank voltage at this time is appropriately reduced so that the total energy of the system is the same as that of the simulation of the conventional PFS. The question of how to achieve the state which serves as our initial simulation condition is deferred for later investigation.

The implosion load is a 2 cm tall, 300 μg/cm^2 cylindrical aluminum foil. The total mass is somewhat less than 20 mg. In place of a 1.11 micron thick solid foil of aluminum, the foil is modeled as a 900 micron thick fluid of the appropriate density to yield the correct areal mass density. This is necessary to keep the numerical time step for the code large enough to allow the problem to run in a reasonable number of computational cycles.

During the first portion of the MACH2 simulations, the grid follows the switch plasma in a rezoned-Lagrangian fashion. After the switch nears the corner where the gun meets the implosion region, the upper right portion of the grid is fixed in the laboratory frame and the plasma switch moves through the grid in an Eulerian manner. After current is switched to the implosion load, the grid follows the imploding fluid, again in a rezoned Lagrangian way until the center of mass of the load is near the axis. Thereafter, the grid is essentially frozen in the lab frame for the final stages of the implosion.

Switching Characteristics

Figure 3 shows MACH2 snapshots of mass density isocontours and fluid velocity vectors for a simulation of a conventional PFS at 3.0 μs. The load gates open to some extent as the supersonic flow around the corner of the switch is guided to the bottom of the foil by the high density switch mass that is left on the inner electrode and that is driven around the corner of the switch. This mass shields the top of the implosion load so magnetic pressure behind the load is greater at the bottom than at the top. Some of the switch mass also accumulates at the bottom of the implosion region and shields the very bottom of the load. This shielding of current creates a 100 ns spread over which current is delivered to the load.

Figure 4 shows the magnetic probe data for the conventional PFS simulation. Essentially all of the current produced by the bank, 11.5 MA, appears at the probe just outside of the implosion load (probe 7) with a 180 ns rise time. Also shown

in this figure are the currents at 2 probe locations at the same radius as probe 7, but at different axial locations. "L" and "U" mean lower and upper probe locations with respect to probe 7 which is in the middle. The temporal spread between these 3 probes is 100 ns which initiates a large perturbation in the implosion.

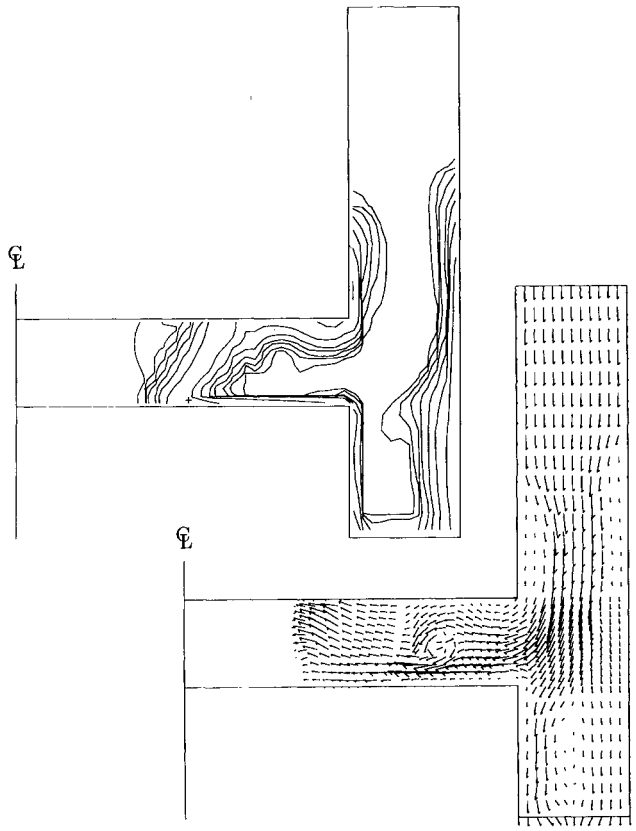

Figure 3. Mass density isocontours and velocity vectors at 3 μsec of a conventional PFS simulation.

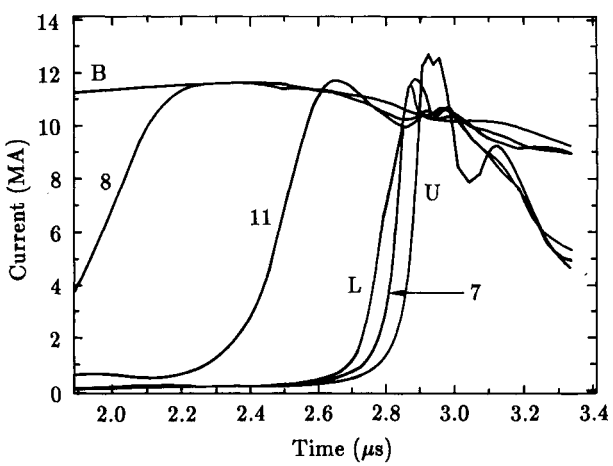

Figure 4. Magnetic probe data for the conventional PFS.

Figure 5 shows MACH2 snapshots of rA_θ (poloidal magnetic flux lines) and mass density isocontours for a simulation of a CT PFS at 0.5 μs. These snapshots illustrate the switching of the CT PFS as torodial magnetic energy is delivered to the implosion load. Figure 6 at 0.8 μs shows that a circulating flow shields the top of the implosion foil from convected magnetic energy which is preferentially delivered to the bottom of the load at later times. There is very little switch plasma in the gun after the CT has moved past the gap that opens to the implosion load. The resulting current delivery is illustrated in Figure 7 where magnetic probe data for the CT PFS simulation is displayed. As with the conventional PFS, essentially all of the current produced by the bank appears at the probe just outside of the implosion load (probe 7). However, this is merely 9 MA—somewhat less than the 11.5 MA delivered by the conventional PFS. The reason for the smaller current is the larger $\dot{L}$ associated with the CT switch. In these simulations, the CT accelerated from an initial speed that is already higher than the final speed of the conventional PFS armature. Figure 7 also shows that the current at the 3 probe locations immediately inside the implosion foil driven by a CT PFS rise with a 40 ns temporal spread—40% of the spread imposed by the conventional PFS. The rise time is 140 ns—75% of the conventional switch.

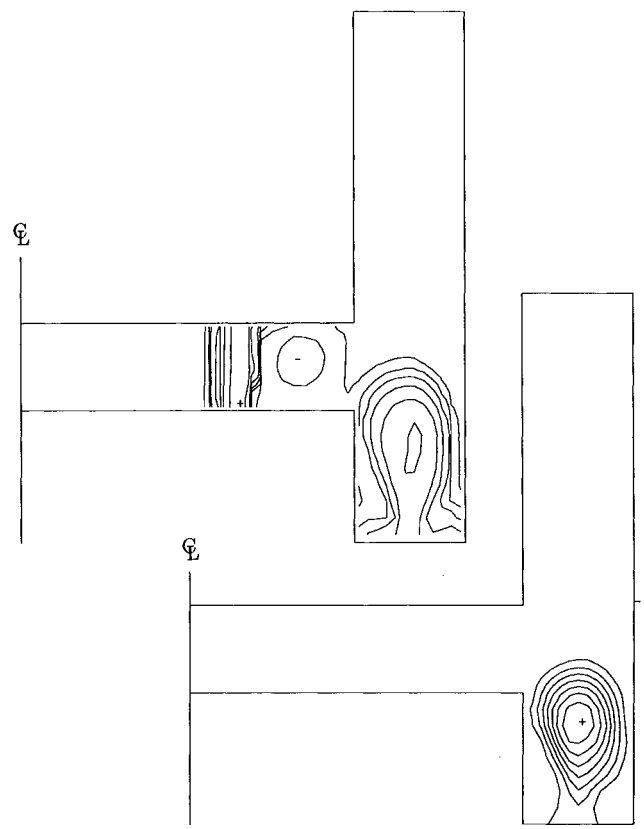

Figure 5. Mass density (above) and rA_θ (below) isocontours of a CT PFS at 0.5 μsec.

Radiated Energy

The nonuniform implosion of the load foil limits the peak radiated power. If the foil remained cylindrically symmetric during the implosion, the power radiated upon stagnation would be on the order of $P_{max} = \epsilon\, Ev/\delta r$, where ϵ is an effectiveness factor: $0 < \epsilon < 1$, E is the energy of the foil, v is its foil speed, and δr its thickness. For 1 MJ delivered to the load foil, $P_{max} \sim \epsilon \times 20$ TW. The configuration of an imploding

foil pushed by a magnetic pressure gradient is Rayleigh-Taylor unstable at the interface between the magnetic field and the foil. The instability effectively increases the foil thickness and reduces the peak power. Whatever can be done to reduce the natural tendency of the implosion foil to disassemble should be done if one desires to increase the radiated power.

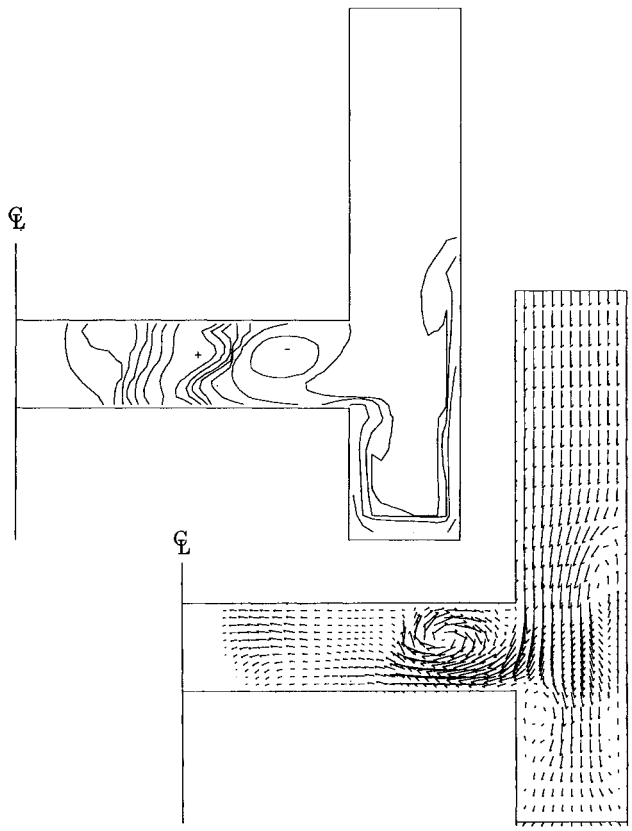

Figure 6. Mass density isocontours and velocity vectors at 0.8 μsec of the CT PFS.

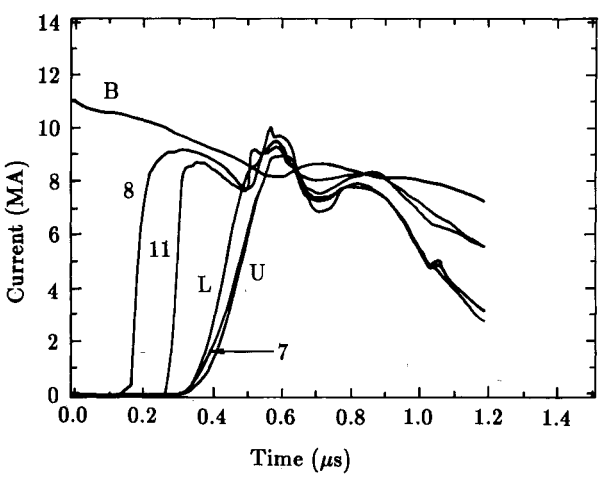

Figure 7. Magnetic probe data for a CT PFS.

The conventional PFS and the present geometry have been thoroughly developed and optimized for extracting power from the Shiva Star bank.[10] The mass left along the walls of the plasma gun by a conventional PFS is one of the perturbations that encourages nonuniform foil implosion. The present CT PFS simulation suggests that this perturbation can be removed if the switch is confined by a magnetic "bag" moving faster than its Alfvén speed. The questions now are: has this improved the symmetry of the implosion, and what is the effect on the radiated power?

Figure 8 shows the radiated power as a function of time for both the conventional and CT PFS simulations discussed above. The time scales for each have been shifted so that the curves can be clearly compared. Approximately 350 kJ has been radiated and the average radiated power is comparable. Because the CT switch crosses the gap to the implosion region faster than the conventional switch, little switch mass is driven into the gap. This means that the energy is coupled entirely to the load foil rather than shared between the load and switch mass in the implosion region. The increased energy per unit mass then drives a faster implosion which yields higher temperatures in the CT case. There is an intriguing narrow peak near 4 TW from the CT PFS-driven implosion that is absent from the conventional PFS-driven implosion. The higher power is produced by the higher temperature of the stagnating load driven by the faster CT switch.

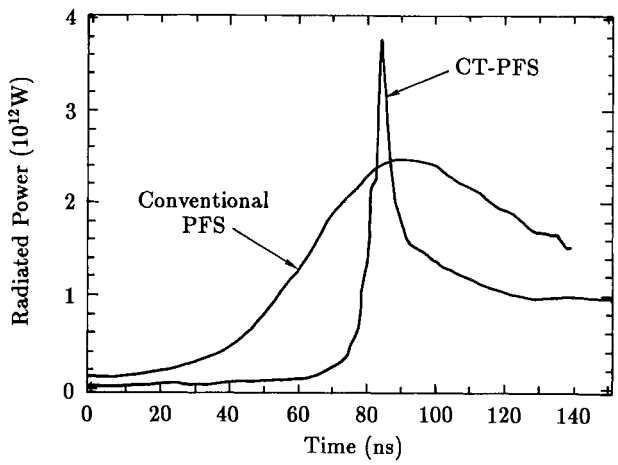

Figure 8. Radiated power from conventional and CT PFS-driven implosions.

Summary

It has been shown that if a CT PFS could be produced with the conditions ascribed to it at the beginning of our numerical simulation, it is capable of delivering current with a 40 ns top to bottom spread to a 2 cm tall implosion foil without leaving switch mass along the walls of the gun and implosion region. The resulting implosion of a 300 μg/cm^2 Al cylindrical foil is at least as efficient at producing radiation in the 3 TW range as a conventional PFS-driven implosion, and it exhibits a sharp peak at 4 TW that is absent from the conventional case.

If it were possible to operate a conventional PFS at the same high current, low mass, and high speed used here for the CT PFS, computer simulations indicate that similar switch performance and implosion quality would be obtained. However, the discharge behind a low mass conventional plasma armature will rapidly increase its speed, and this will add a large impedance to the circuit. The large impedance will generally

prevent the current from reaching a desired large value. In addition, computer simulations show that the plasma of a conventional switch, unconfined by self-magnetic fields, tends to pitch open toward the outer electrode if the acceleration time is too long. In general, a PFS performs poorly if switch mass remains in the gun while current is delivered to a load. The discharge behind a CT armature, however, can push it into a compression cone where the self-magnetic confinement will limit the early plasma motion and hence the circuit impedance. A low impedance CT armature will therefore permit high currents to be obtained prior to high speed switching.

The present geometry and foil mass are chosen to optimize the radiation output of the conventional PFS. It is possible that increased radiation yield would be obtained by optimizing the configuration for the CT case. The results of this paper are sufficiently promising to warrant further computational investigation into the usefulness of a compact torus PFS.

This work is supported by the Phillips Laboratory, Air Force Systems Command.

References

[1] K. E. Hackett, *et al.*, "Megagauss Magnetic Field Production Using Compact Toroidal Plasmas," in Megagauss Fields and Pulsed Power Systems, V. M. Titov and G. A. Svetsov, eds., (Nova Science Publishing, NY, NY 1990).

[2] W. L. Baker, *et al.*, "Plasma Flow Switch Driven Liner Implosions," *Megagauss Fields and Pulsed Power Systems* V. M. Titov and G. A. Shvetsov, eds., pp. 615–622, (Nova Sciences Publishers, New York, NY, 1990).

[3] W. L. Baker, "Multi-Megampere Plasma Flow Switch Driven Liner Implosions," *MegaGauss Technology and Pulsed Power Applications* C. M. Fowler, R. S. Caird, and D. J. Erickson, eds., pp. 652–653, (Plenum Press, New York, NY, 1987).

[4] P. J. Turchi, *et al.*, "Development of Coaxial Plasma Guns for Power Multiplication at High Energy," *Digest of Technical Papers: Third IEEE International Pulsed Power Conference* T. H. Martin and A. H. Guenther, eds., pp. 455–462, 1–3 June 1981, Albuquerque, NM, (IEEE, New York, NY, 1981).

[5] P. J. Turchi, "Magnetoacoustic Model for Plasma Flow Switching," *Digest of Technical Papers: Fourth IEEE Pulsed Power Conference* M. F. Rose and T. H. Martin, eds., pp. 342–345, 6–8 June 1983, Albuquerque, NM, (IEEE, New York, NY, 1983).

[6] W. L. Baker, *et al.*, "QUICK-FIRE Plasma Flow Driven Implosion Experiments," *Digest of Technical Papers: Fifth IEEE Pulsed Power Conference* M. F. Rose and P. J. Turchi, eds., pp. 728–731, 10–12 June 1985, Arlington, VA, (IEEE, New York, NY, 1985).

[7] J. Buff, *et al.*, "Simulations of a Plasma Flow Switch," *IEEE Transactions on Plasma Science* PS-15 (6), pp. 766–771 (1987).

[8] J. H. Degnan, *et al.*, "Experimental Results from SHIVA STAR Vacuum Inductive Store/Plasma Flow Switch Driven Implosions," *IEEE Transactions on Plasma Physics* PS-15 (6), pp. 760–765 (1987).

[9] J. Buff, *et al.*, "Enhancement of the Radiation Yield in Plasma Flow Switch Experiments," *IEEE Trans. on Plasma Science* Vol. 19 (3), (1991).

[10] R. E. Peterkin, Jr., A. J. Giancola, M. H. Frese, and J. Buff, "MACH2: A Reference Manual—Fourth Edition," MRC/ABQ-R-1207, Mission Research Corporation, November 1989.

[11] M. H. Frese, "MACH2: A Two-Dimensional Magnetohydrodynamic Simulation Code For Complex Experimental Configurations," AMRC-R-874, updated March 1990.

[12] P. J. Turchi, *et al.*, "Review of Plasma Flow Switch Development," *IEEE Transactions on Plasma Science* PS-15 (6), p. 747 (1987).

[13] A. W. Molvik, *et al.*, "Quasistatic Compression of a Compact Torus," *Phys. Rev. Lett.* 66, p. 165 (1991).

[14] C. R. Sovinec, *et al.*, *Bull. Am. Phys. Soc.* 35, p. 2059 (1990).

[15] R. E. Peterkin, Jr., *et al.*, *Bull. Am. Phys. Soc.* 35, p. 2059 (1990).

[16] C. R. Sovinec, *et al.*, "MARAUDER Computer Simulations with Two Toroidal Field Circuits," *IEEE Conference Record—Abstracts, 1991 ICOPS*, pp. 167–168, 3–5 June 1991, Williamsburg, VA (IEEE, New York, NY, 1991).

[17] M. Abramowitz and I. A. Stegun, *Handbook of Mathematical Functions*, (Dover Publications, Inc., New York, NY) p. 374 (1970).